Performance of quantum-dash mode-locked lasers (QD-MLLDs) for high-capacity coherent optical communications

Khalil, Mostafa; Xie, Yuxuan; Berikaa, Essam; Liu, Jiaren; Lu, Zhenguo; Poole, Philip J.; Liu, Guocheng; Weber, John; Plant, David V.; Chen, Lawrence R.

Publisher's version / Version de l'éditeur:
https://doi.org/10.1364/OE.509643
Optics Express, 32, 1, pp. 217-229, 2024

Research Article Vol. 32, No. 1 / 1 Jan 2024 / Optics Express 217
Optics EXPRESS

Performance of quantum-dash mode-locked lasers (QD-MLLDs) for high-capacity coherent optical communications

MOSTAFA KHALIL,[1,*] YUXUAN XIE,[1] ESSAM BERIKAA,[1] JIAREN LIU,[2] ZHENGUO LU,[2] PHILIP J. POOLE,[2] GUOCHENG LIU,[2] JOHN WEBER,[2] DAVID V. PLANT,[1] AND LAWRENCE R. CHEN[1]

[1]*Electrical and Computer Engineering Department, McGill University, Montreal, H3A 0E9, QC, Canada*
[2]*Advanced Electronics and Photonics Research Center, National Research Council Canada, Ottawa, K1A 0R6, ON, Canada*
[*]*mostafa.khalil2@mail.mcgill.ca*

Abstract: We investigate the capabilities and limitations of quantum-dash mode-locked lasers (QD-MLLDs) as optical frequency comb sources in coherent optical communication systems. We demonstrate that QD-MLLDs are on par with conventional single-wavelength narrow linewidth laser sources and can support high symbol rates and modulation formats. We manage to transmit 64 quadrature amplitude modulation (QAM) signals up to 80 GBd over 80 km of standard single-mode fiber (SSMF), which highlights the distinctive phase noise performance of the QD-MLLD. Using a 38.5 GHz (6 dB bandwidth) silicon photonic (SiP) modulator, we achieve a maximum symbol rate of 104 GBd with 16QAM signaling and a maximum net rate of 416 Gb/s per carrier in a single polarization setup and after 80 km-SSMF transmission. We also compare QD-MLLD performance with commercial narrow-linewidth integrable tunable laser assemblies (ITLAs) and explore their potential for use as local oscillators (LOs) and signal carriers. The QD-MLLD has 45 comb lines usable for transmission at a frequency spacing of 25 GHz, and an RF linewidth of 35 kHz.

1. Introduction

In the ever-evolving demand for high-speed data transmission to serve long-haul networks, data-center interconnects and metropolitan networks, the demand for robust and scalable communication systems has been growing rapidly [1]. One of the keys to meeting this demand lies in the effective utilization of wavelength-division multiplexing (WDM), a technique that enables multiple data streams to be transmitted over the same optical channel. As optical communication networks evolve, there is a growing need for compact and highly efficient WDM transceivers capable of handling multi-Tb/s connectivity with ease [2,3]. The emergence of optical frequency combs stands out as a compelling solution for high-capacity coherent optical transmission. Quantum dash mode-locked laser diodes (QD-MLLDs) have attracted significant attention for coherent optical communications due to their compact size, simple operation, and the ability for hybrid integration with silicon substrates [4]. QD-MLLDs have the capability to emit broadband frequency combs composed of tens of evenly spaced optical carriers with a relatively flat spectral envelope [5,6]. Thanks to their narrow optical linewidth [5], usually tens of kHz to a few MHz, these comb sources allow employing higher order modulation formats.

In recent years, several chip-scale comb generators have demonstrated their ability to facilitate high-speed WDM transmission at Tbit/s data rates. Among these, the so-called Kerr microring resonator [7,8], utilizing the Kerr nonlinearities within optical waveguides, can generate hundreds of comb lines over a large bandwidth span of 10 THz or more, and are usable for data transmission [9,10]. Coherence-cloned Kerr solitons also offer stability in frequency and phase of the carriers

#509643 https://doi.org/10.1364/OE.509643
Journal © 2024 Received 17 Oct 2023; revised 6 Dec 2023; accepted 8 Dec 2023; published 18 Dec 2023

Optics EXPRESS

over long distances, enabling unique advantages in digital signal processing (DSP). In [11,12], the authors showcased the regeneration of dissipative Kerr soliton microcombs with strong coherence, enabling them to function as both transmitter carriers and receiver local oscillators (LOs) for high-speed data transmission. The efficiency of Kerr microring resonators can vary widely depending on several factors, such as the quality factor, the nonlinear coefficient, and the loss of the microring resonator, as well as the pump power, the pump wavelength, and the channel spacing. Their fabrication and tuning can be complex, requiring precise control over parameters such as temperature, optical power, and cavity length. Achieving frequency spacing between comb lines at higher symbol rates can also pose challenges. Microring resonators, in general, are sensitive to environmental variations, affecting their stability in practical applications. The Gaussian-shaped output spectrum implies varying extinction ratios among the comb lines, impacting uniformity. Another method for comb generation is by relying on gain switching of injection-locked distributed feedback (DFB) lasers. Although these can be integrated into chip-scale packages, they suffer from the limited bandwidth, typically spanning less than 500 GHz [13,14]. Cascaded Mach-Zehnder modulators (MZMs) have been demonstrated over the years for frequency comb generation [15,16]; however, the setup requires RF signal generators and additional RF amplifiers and is limited by the modulator bandwidth and the frequency of the RF signal generator [16]. QD-MLLDs overcome these limitations and offer a broadband comb-line spectrum requiring only a simple DC current [17,18]. In addition, QD-MLLDs have no optical coupling interfaces that cause loss and reduce the efficiency. Table 1 provides a summary of recent findings regarding the utilization of QD-MLLDs in coherent optical transmission systems. The highest recorded symbol rate using these lasers is 45 GBd, achieved with 4-quadrature amplitude modulation (QAM) signaling [19]. It is important to note that the primary objective of our study is not merely to establish new records, e.g., in terms of transmission data rate, but rather to explore thoroughly the limitations and capabilities of QD-MLLDs in coherent optical communications. Specifically, we aim to investigate the upper bounds of modulation formats and symbol rates that these lasers can successfully support. The QD-MLLD used in this study is fully packaged and does not need any stabilization or optical feedback locking [20,21].

Table 1. Summary of some of the reported QD-MLLD used for coherent data transmission

Ref	# of comb lines	Frequency spacing [GHz]	Symbol rate [GBd]	Aggregate bitrate	Modulation format	Fiber length [km]	BER	Single/ dual Pol.
This work	10	100	96	1.92 Tb/s	4QAM	80	$< 3.8 \times 10^{-3}$	Single
	1	-	80	480 Gb/s	64QAM		$< 2 \times 10^{-2}$	
[25]	52	28.4	32	256 Gb/s	16QAM	B2b	$< 2 \times 10^{-2}$	Dual
[17]	56	28.4	28	12.5 Tb/s	16QAM	100	$< 3.8 \times 10^{-3}$	Dual
[26]	48	34.2	28	10.8 Tb/s	16QAM	100	$< 1.6 \times 10^{-2}$	Dual
[27]	48	34.2	28	5.4 Tb/s	PAM4	25	$< 1.6 \times 10^{-6}$	Dual
[28]	12	25	18	800 Gb/s	16QAM	78	$< 2 \times 10^{-3}$	Single
[19]	23	50	45	4.14 Tb/s	4QAM	75	$< 1 \times 10^{-9}$	Dual
[6]	38	42	38	11.55 Tb/s	16QAM	75	$< 1.4 \times 10^{-2}$	Dual
[5]	47	34.36	32	12 Tb/s	16QAM	B2b	$< 3.8 \times 10^{-3}$	Dual
[29]	50	40	25	100 Gb/s	4QAM	10	$< 3.8 \times 10^{-3}$	Dual
[30]	60	25	20	12 Tb/s	32QAM	75	$< 4.4 \times 10^{-3}$	Dual
[31]	36	34.5	12.5	1.8 Tb/s	4QAM	50	$< 4 \times 10^{-3}$	Dual
[32]	25	42	18	1.56 Tb/s	16QAM	75	$< 1 \times 10^{-2}$	Single
[33]	4	100	28	112 Gb/s	OOK	100	$< 1 \times 10^{-9}$	-

Optics EXPRESS

Concurrently, silicon photonic (SiP) devices have gained considerable attention due to their cost-effectiveness and compatibility with complementary metal-oxide semiconductor (CMOS) processing [22]. Numerous studies have showcased the exceptional performance of SiP MZMs in coherent communications, enabling Tb/s applications ideal for both long-haul and data center transmissions [23,24].

With these factors in mind, this paper delves into a comprehensive exploration of QD-MLLDs and their performance in coherent transmission systems. Our investigation begins with an in-depth analysis of the comb source characteristics, encompassing parameters such as linewidth, relative intensity noise (RIN), frequency spectrum, and phase noise. Subsequently, we assess their transmission performance for different symbol rates and modulation formats using a testbed with practical bandwidth limitations. Furthermore, our investigation includes the performance of 45 channels (6 dB bandwidth) generated from the comb source, which can be used for data transmission.

In this evaluation, nearly uniform performance is observed across all channels, with minor variations occurring primarily for the comb lines located at the edges of the comb spectrum with lower output power. Additionally, we conduct a WDM transmission experiment, where we program the comb spectrum to select 10 comb lines with 100 GHz spacing. These carriers are modulated at 4QAM with a symbol rate of 96 GBd. The outcomes of this endeavor underscore the QD-MLLD's versatility, as it demonstrates robust performance at 4QAM 112 GBd and 16QAM 104 GBd signaling, consistently achieving bit error ratio (BER) values below the hard decision (HD)-FEC and soft-decision (SD)-FEC thresholds following an 80 km standard single-mode fiber (SSMF) transmission. In our pursuit of evaluating the performance of the QD-MLLD, we compare its performance with integrable tunable laser assemblies (ITLAs). The results of this comparison reveal that the QD-MLLD is a potential competitor in high-speed data transmission applications. Furthermore, we explore the feasibility of employing QD-MLLDs as LOs and/or signal carriers [19], substantiating these investigations through optical signal-to-noise power ratio (OSNR) measurements. Lastly, our study delves into the compatibility of QD-MLLDs with single-segment in-phase and quadrature (IQ) SiP modulators. This exploration opens exciting prospects for future hybrid integration between silicon photonics and QD-MLLDs, potentially unlocking innovative possibilities in optical transceiver modems.

2. Characteristics of the QD-MLLD comb source

The design of the QD-MLLD used in this work is depicted in Fig. 1(a). The QD-MLLD is a specialized InP-based p-n blocked buried heterostructure Fabry-Perot (FP) laser. The core of the laser structure comprises a 170 nm thick indium gallium arsenide phosphide (InGaAsP) waveguide with 10 nm $In_{0.816}Ga_{0.184}As_{0.392}P_{0.608}$ (1.15Q) barriers that encase five layers of InAs QDashes, serving as the active gain region. These layers are surrounded by cladding layers of both n- and p-type InP material. The n-type InP cladding includes 1.03Q ballast layers, optimizing the laser's optical performance. The InAs QDash material was grown using chemical beam epitaxy (CBE) and underwent additional processing through metal-organic chemical vapor deposition (MOCVD) to create the buried heterostructure. Each active layer had an average QDash density of around $1.5 \times 10^{10}\,\mathrm{cm}^{-2}$. The laser's 1735 µm long waveguide was crafted using standard photolithography techniques, involving dry and wet etching, and contact metallization. A 2 µm wide waveguide mesa was formed to confine the current. The laser chip was mounted on a commercially available aluminum nitride (AlN) carrier with gold electroplated contacts and packaged into a standard 14-pin butterfly laser diode as shown in Fig. 1(a) inset. The temperature of the QD-MLLD is controlled by a thermoelectric cooler (TEC) and biased by a laser diode controller (LDC). The QD-MLLD exhibits a lasing threshold at approximately 50 mA and can achieve an average output power of 50 mW when operated at a bias current of 450 mA. At this

Optics EXPRESS

operating point, its 6 dB optical bandwidth extends to approximately 9 nm, and it produces over 50 comb lines with a comb spacing of 25 GHz.

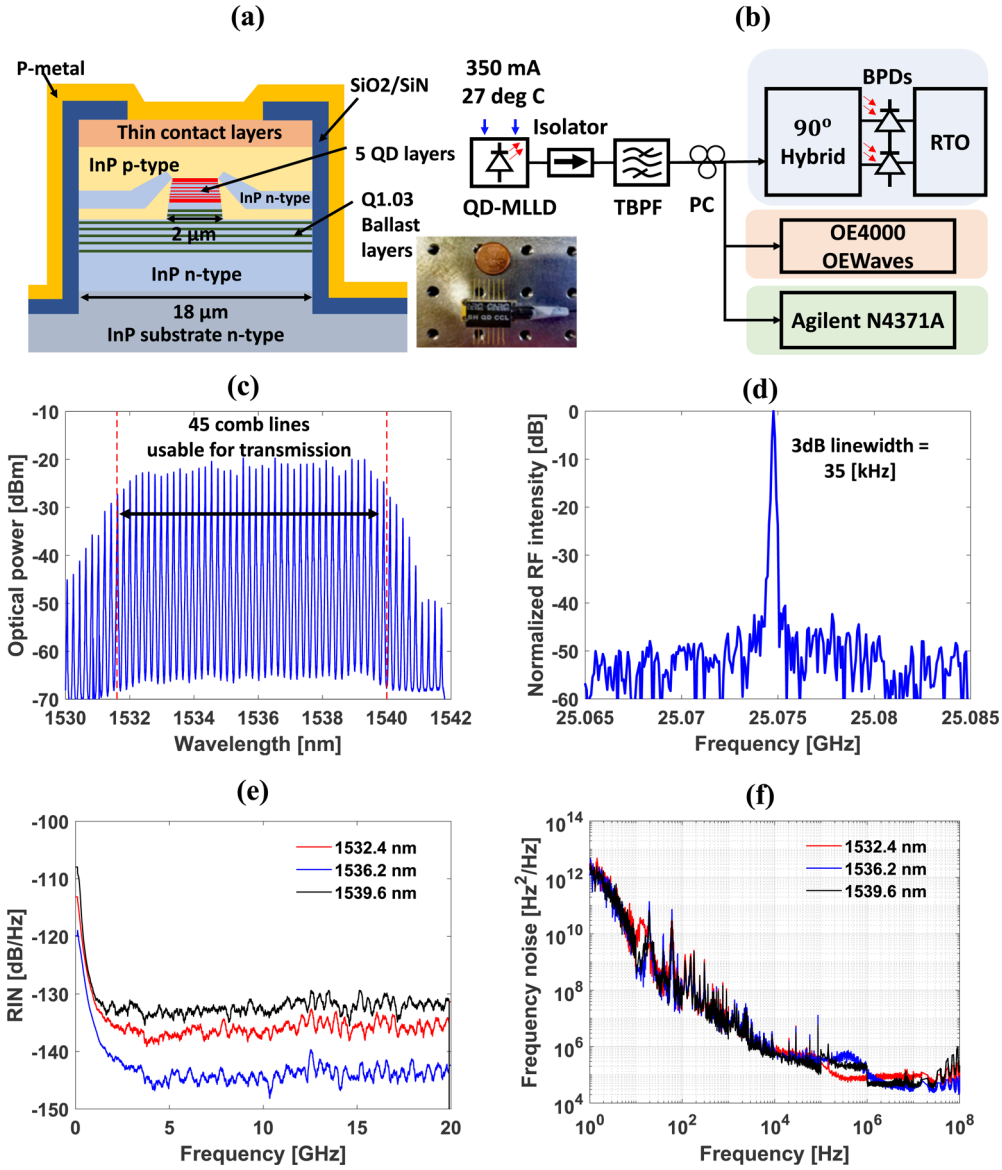

Fig. 1. (a) Schematic design of the QD-MLLD, the inset shows a picture of the QD-MLLD after packaging. (b) Experimental setup used to characterize the QD-MLLD. (c) The output optical spectrum of the QD-MLLD with resolution of 10 pm. (d) Linewidth measurement of the QD-MLLD highlighting a 3-dB RF linewidth of 35 kHz, at free spectral range (FSR) of 25 GHz indicating the frequency spacing between the comb lines. (e) RIN measurements of 3 comb lines selected in the beginning, the middle, and the end of the comb spectrum. (f) Frequency noise measurements of the 3 selected comb lines.

To investigate the characteristics of the QD-MLLD source, we conducted a comprehensive assessment of the device using different setup configurations as illustrated in Fig. 1(b). We set the operating current at 350 mA and the temperature was set at 27°C using a LDC (ILX Lightwave

Optics EXPRESS

LDC-3900). This deliberate temperature choice was made to shift the comb spectrum towards the C-band. While it was possible to increase the temperature further to observe additional shifts towards the mid of the C-band, operating at higher temperatures for prolonged period of time is not advisable as it may reduce the lifetime of degrade the performance of the devices. For the safety and optimal functioning of the device, we maintained it at room temperature. At these operating conditions, there are 45 comb lines (6 dB bandwidth) that are usable for coherent transmission, and the comb lines exhibit optical carrier-to-noise power ratios (OCNR) to be more than 40 dB as shown in Fig. 1(c).

An isolator is used to protect the device from potential back reflections within the system. It is followed by a tunable band-pass filter (TBPF) (Santec OTF-350) to select two or more carriers from the comb source. The selected carriers are then directed through a polarization controller (PC) and launched into a 90° optical hybrid. At the output of the optical hybrid, balanced photodetectors (BPD) (Finisar 43 GHz) followed by a 160 GSa/s real-time oscilloscope (RTO) (Keysight 2 channels, 63 GHz bandwidth, 8-bit resolution) are used to capture the in-phase and quadrature component of the beat signal. Figure 1(d) shows the measured RF linewidth with respect to the beating RF note at roughly 25 GHz, namely, the frequency spacing between the comb lines. The 3-dB RF linewidth is measured to be around 35 kHz indicating that the comb tones are closely synchronized and coherent which is essential for reliable data transmission and enhancing signal quality [34,35]. Narrow RF linewidths indicate strong phase correlation between the cavity modes and is an indirect measurement of the comb line linewidth. The RF linewidth gives a maximum value for the instantaneous comb linewidth. The RF linewidth can further be narrowed into a few kHz by optimizing the waveguide structure and the self-injection technology, or by using optical feedback loop from an external cavity as demonstrated in [36,37]. The transmission performance of each comb line is dependent on its RIN, optical linewidth, and signal-to-noise ratio (SNR). A larger RF linewidth means more phase noise, which increases the overall BER, and degrades the transmission performance.

Moreover, to characterize the noise performance of the device, we employed an automated laser linewidth and phase noise measurement system (OE4000 OEWaves Inc.) to measure the optical frequency-noise of the selected individual. The RIN is measured using a RIN measurement system (Agilent N4371A) and the integrated RIN for the selected individual channels over a frequency range of 10 MHz to 20 GHz is calculated between -130.7 dB/Hz and -145.2 dB/Hz as shown in Fig. 1(e), while the frequency-noise spectra are shown in Fig. 1(f). The three wavelengths shown in Fig. 1(e) were chosen for illustrative purposes across the comb spectrum. For RIN performance, we observed the typical parabolic-like behavior as a function of wavelength. Specifically, the RIN shows an increase for the comb lines situated at the spectral edges. The lowest RIN (blue curve) corresponds to one of the channels located in the middle of the spectrum, whereas the red and black curves represent the channels at both the left and right edges. This happens because the extinction ratio of the comb lines on the edges are lower compared to the ones in the middle, and they have more power fluctuations. Frequency-noise components below 100 MHz are typically mitigated through phase tracking techniques in the DSP, while spectral components exceeding 100 MHz can potentially deteriorate signal quality [6].

3. Coherent transmission using QD-MLLDs

We highlight the capabilities of QD-MLLDs in coherent WDM transmission, showcasing their performance at high modulation formats and symbol rates over 80 km of SSMF. We perform a semi super-channel transmission over 80 km of SSMF by modulating 10 comb lines at 100 GHz spacing with a 8 GHz guard band (4 GHz on each side). Additionally, we conduct a performance comparison between the QD-MLLD and ITLA, demonstrating that the QD-MLLD is a competitive candidate for high-speed coherent transmissions. Moreover, we demonstrate the potential of such

Optics EXPRESS

comb sources for hybrid-integration with silicon photonics. We use the comb source to perform coherent transmissions with an on-chip silicon photonic modulator over 80 km of SSMF.

3.1. Performance analysis of the QD-MLLD

Figure 2(a) illustrates the experimental setup and the DSP routine employed in the system. At the transmitter, we generate the desired symbols for the QAM order. These symbols then undergo two essential steps: upsampling and pulse shaping, which are accomplished using a root raised cosine (RRC) filter featuring a 2% roll-off factor. The arbitrary waveform generator (AWG) (Keysight M8199A) employed in this process boasts a substantial output swing capacity, reaching up to 830 mVpp, and maintains high signal fidelity throughout. Following these preparations, the RF signals are loaded into the SHF QAM transmitter (SHF 46213D, single polarization) equipped with integrated RF amplifiers. To ensure precise control over the modulated signal, the biasing of the IQ modulator within the SHF QAM transmitter is manually adjusted.

On the optical side, after the comb source, an isolator is employed to safeguard the device against potential back reflections generated within the system. Subsequently, a tunable band-pass filter (TBPF) is used to select a single comb line or multiple comb lines. Following this, an erbium-doped fiber amplifier ($EDFA_1$) is used to boost the total power of the comb source to 16 dBm, aligning with the maximum optical input power requirement for the SHF QAM transmitter. A polarization controller (PC) is used as the SHF QAM transmitter is a single polarization device. The total number of comb lines that can be used for transmission is 45 comb lines. To control the spacing between the comb lines, a programmable optical filter (Finisar 1000s) is used, e.g., to select 10 comb lines with a frequency spacing of 100 GHz. After modulation, optical launch power optimization is carried out using $EDFA_2$ (Oclaro PG2800) to prevent nonlinearities before sending the signal across an 80 km span of SSMF. Given an approximate 17 dB fiber loss in the channel, $EDFA_3$ is employed to compensate for this loss. The signal is subsequently directed into a 90-degree hybrid and combined with an ITLA functioning as a LO. The outputs of the optical hybrid are detected by 43 GHz balanced photodiodes (BPD), followed by analysis with a 160 GSa/s real-time oscilloscope (RTO) (Keysight DSOX96204Q). To meet our experimental requirements, we utilize the RTO's 2 channels with a bandwidth of 63 GHz. The received signals are subsequently processed offline.

Within the receiver's DSP, we apply Gram-Schmidt orthogonalization [38] to rectify any imperfections that may arise from the hybrid. Then, we resample the signals to 2 samples per symbol (sps) for compensating for chromatic dispersion (CD) [39] and correcting frequency offset (FO). Following this, synchronization is performed using a cross-correlation between the received symbols captured by the RTO and the training symbols. To enhance the SNR, we employ a RRC matched filter. To mitigate linear distortion and phase noise, we utilize a second order phase locked loop (PLL) [40] that is included within the adaptive blind equalizer based on the least mean squares (LMS) algorithm. Eventually, the recovered symbols are de-mapped to bit sequence for BER calculations.

First, we select a single comb line at around 1536.2 nm (in the middle of the comb spectrum) for our symbol rate sweep analysis. The programmable optical filter is used to filter out any unwanted amplified spontaneous emission (ASE) noise and to guarantee that no additional comb lines were introduced into the modulator. Figure 2(b) shows the measured bit error ratios (BER) across various symbol rates, encompassing four distinct modulation formats, ranging from 4QAM to 64QAM. The dashed lines represent the back-to-back (B2B) data transmission results. The summary of the achieved transmission net rates is presented in Table 2. We achieved a modulation format of 64QAM at 80 GBd with a BER below the 25% overhead (OH) SD-FEC threshold after 80 km-SSMF transmission. At 4QAM signaling, we accomplished a 112 GBd transmission rate over the same 80 km-SSMF distance. These results are primarily limited by the bandwidth limitations from the SHF QAM transmitter and BPDs.

Optics EXPRESS

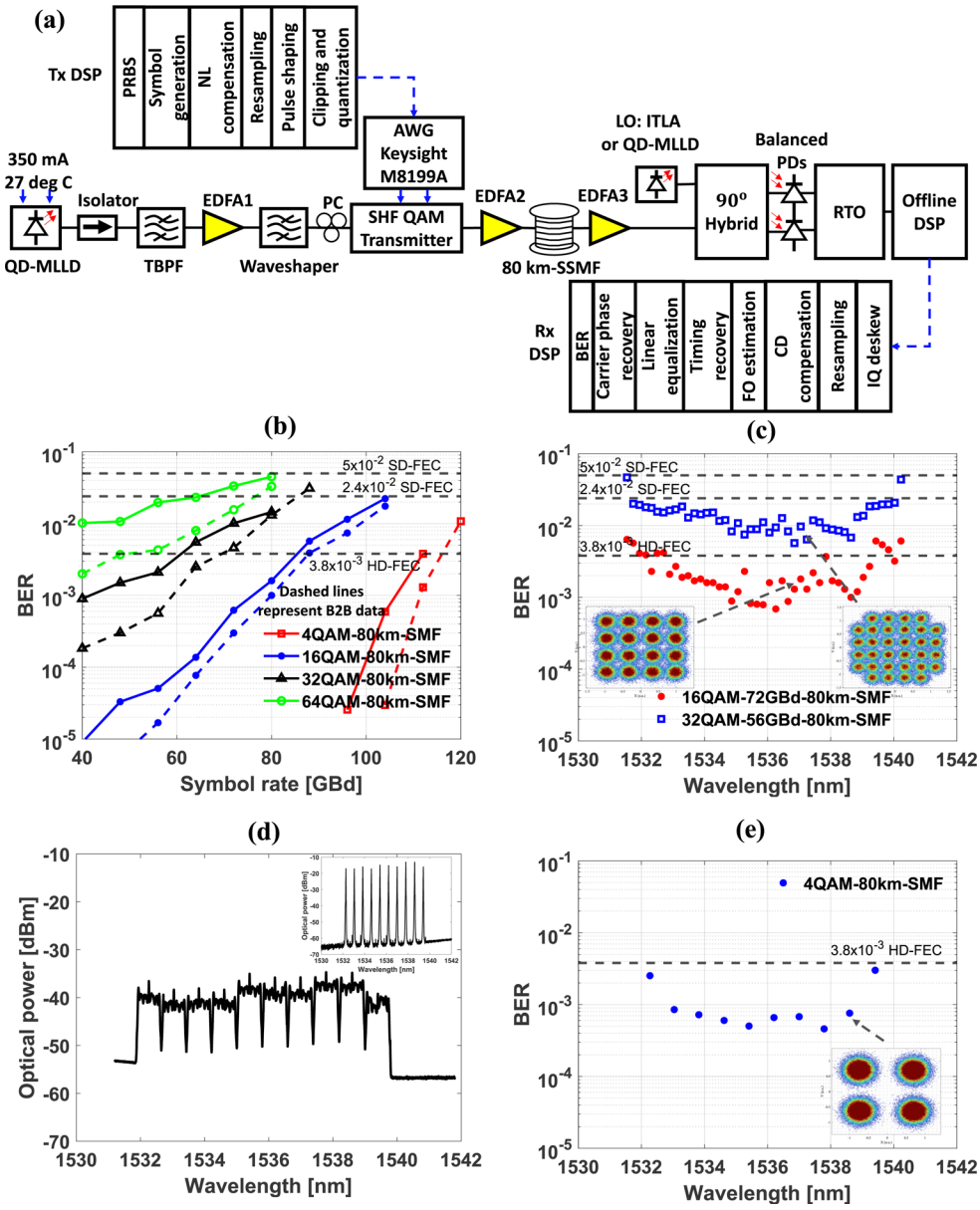

Fig. 2. (a) Experimental setup for the coherent transmission experiment with the SHF QAM transmitter, and DSP routine used in both the transmitter and receiver. (b) BER as a function of symbol rate for one of the channels of the QD-MLLD with modulation formats ranging from 4 to 64QAM. (c) BER as a function of wavelengths of the 45 channels usable for transmission over 80 km-SSMF using 16QAM at 72GBd (red dots) and 32QAM at 56GBd (blue squares). (d) Comb spectra of the 10 channels before modulation (inset) and after transmitting over 80 km-SSMF. (e) BER of the 10 transmitted channels with 100 GHz spacing using 4QAM at 96 GBd modulation signal, the inset shows the constellation diagram of one of the channels.

Next, we demonstrate the performance of the individual channels from the comb source. Figure 2(c) shows a comprehensive view of the measured BER for all 45 channels. We

Optics EXPRESS

Table 2. Summary of net bitrate after 80 km-SSMF transmission for a single comb line on a single polarization

BER threshold	FEC OH	Modulation format	Net bitrate [Gb/s]
3.8×10^{-3}	6.7%	112 GBd 4QAM	111.1
		85 GBd 16QAM	338.7
		60 GBd 32QAM	298.8
2.4×10^{-2}	20%	104 GBd 16QAM	332.8
		80 GBd 32QAM	320
5×10^{-2}	25%	80 GBd 64QAM	447.8

employ 16QAM at 72 GBd signaling and 32QAM at 56 GBd signaling; the inset highlights the constellation diagrams of the corresponding data points. For 16QAM signaling, the majority of the BER values falls below the 6.7% OH HD-FEC threshold. This suggests robust performance and the ability to transmit data at high speeds for almost all channels from the comb source. A noteworthy observation is that there are some challenges at the channels residing on the edges of the comb spectrum. For 32QAM signaling, most BER values remain below the 20% OH SD-FEC threshold. However, there are exceptions – the channels located at both ends of the comb spectrum exhibit slightly higher error rates. The reason behind this behavior can be traced to the fact that these edge channels possess lower peak power-to-noise ratios and higher RIN compared to the channels situated in the middle of the spectrum. Figure 1(e) also highlights that the channels on the edges have higher RIN. To ensure the reliability of our findings, each BER value underwent multiple measurements, and we computed the average BER. This approach ensures that the reported BER values accurately represent the performance of the channels. Despite variations in the modulation formats and symbol rates, the measured BER values across the channels of the comb source exhibit consistent behavior for high-speed data transmission. This consistency is a positive indicator of the comb source's suitability for various communication applications.

Finally, we use the programmable optical filter to select 10 comb lines at 100 GHz frequency spacing. Figure 2(d) shows the 10 modulated comb lines after 80 km-SSMF transmission; the inset shows the comb lines before modulation, with an optical spectrum resolution of 10 pm. For our transmission experiment, we transmit 4QAM at 96 GBd, with a guard band of 8 GHz between the modulated signals. Figure 2(e) shows the BER values of the transmitted WDM channels. All the BER values fall below the threshold of 3.8×10^{-3} accounting for a HD FEC scheme with 6.7% OH. The net bitrate achieved through this approach is 1.79 Tb/s using only a single polarization scheme. In [41], we applied the same technique, utilizing the programmable filter to modulate 20 comb lines with a frequency spacing of 50 GHz at a symbol rate of 50 GBd for both 4QAM and 16QAM, leading to aggregate bitrates of 2 TB/s and 4 Tb/s, respectively. Based on these results, the most significant discovery lies not in the net bitrate itself but in the remarkable capability of the comb source to support symbol rates of nearly 100 GBd over extensive transmission distances. This highlights the comb source's robustness and efficiency in enabling high-speed data transmission, making it a promising technology for future high-capacity communication systems.

3.2. Comparison of the performance between QD-MLLD and ITLA

In this section, we conduct a comprehensive comparison of the performance between the QD-MLLD and a commercial narrow-linewidth external cavity laser ITLA. The optical output power from the QD-MLLD and the ITLA is kept the same for fair comparison, around 14 dBm. We explore scenarios where the QD-MLLD serves as the LO and the ITLA as the signal carrier and vice versa, and compare to the use of separate ITLAs for the LO and signal carrier. Figure 3(a)

Optics EXPRESS

shows the BER values as a function of symbol rate up to 120 GBd for the three scenarios. The results demonstrate that the QD-MLLD and the ITLA exhibit comparable performance. However, when the comb source is used as the LO, there is a slight degradation in performance, which can be attributed to variations in the comb source power. To further assess their performance, we compare the BER as a function of OSNR. For 16 QAM at a symbol rate of 56 GBd, the three cases exhibit roughly similar behavior as shown in Fig. 3(b). However, we can see a degradation in the performance when we use the QD-MLLD as an LO, due to the extra EDFA used to boost the power of a single carrier from the QD-MLLD. In Fig. 3(c), we provide samples of the constellation diagrams for different modulation formats that remain below the FEC thresholds.

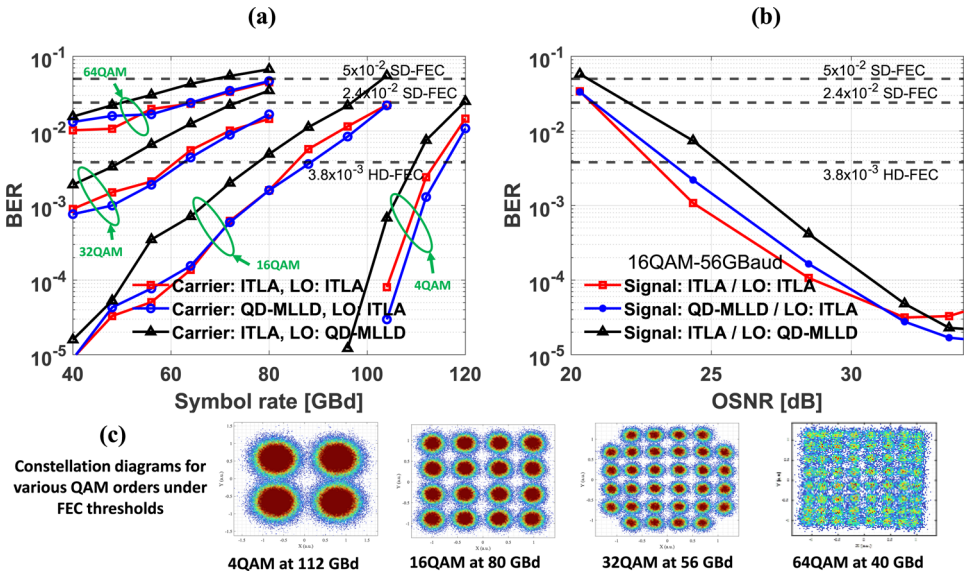

Fig. 3. (a) BER versus symbol rate for different modulation formats in three cases: red (ITLA as carrier and LO), blue (QD-MLLD as carrier and ITLA as LO), and black (ITLA as Carrier and QD-MLLD as LO). (b) OSNR measurement for the three cases at 16QAM 56 GBd. (c) Constellation diagrams for modulation formats from 4QAM to 64QAM.

3.3. Coherent transmission with QD-MLLD and on-chip silicon photonic modulator

We perform coherent transmission with the QD-MLLD and a silicon photonic (SiP) single-segment IQ modulator. The experimental setup is shown in Fig. 4(a). The design and characterization of the SiP have been reported in [24]. Briefly, the SiP is fabricated at the advanced micro foundry (AMF) using a CMOS-compatible process. It consists of two child Mach-Zehnder modulators (MZMs) connected in parallel. Each MZM has phase shifters with a length of 4 mm. The child MZMs are configured for series push-pull configuration, requiring a single RF signal per MZM for operations. The electro-optic (EO) response of the SiP modulator is shown in Fig. 4(b) for different biasing voltages. The modulator has a 3-dB (6- dB) bandwidth of 20 (28.5) GHz without reverse biasing that increases to 28 (38.5) GHz at 3 V reverse bias. The inset shows a microscopic image of the fabricated chip along with the fiber array unit (FAU) and ground-signal signal-ground (GSSG) RF probes used in the experiments. In Fig. 4 we present the outcomes obtained with the SiP modulator. Figure 4(c) shows the BER results across various symbol rates for one of the channels from the comb source.

We achieve symbol rates of up to 88 GBd with 16QAM and 56 GBd with 32QAM, all below the SD-FEC threshold with 20% overhead. We achieve maximum symbol rates of 104 GBd with

Optics EXPRESS

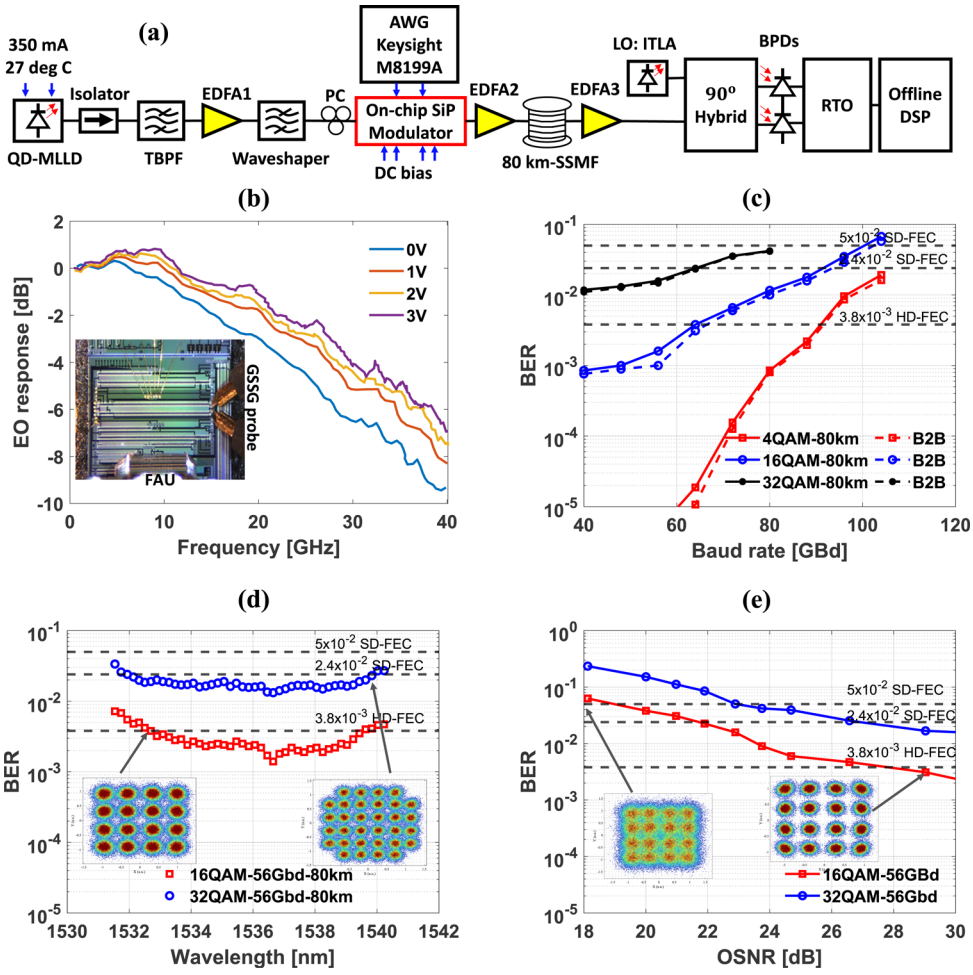

Fig. 4. (a) Experimental setup for the coherent transmission experiment with the SiP modulator. (b) The EO response S_{21} of the SiP modulator, the inset is a microscopic image of the SiP chip. (c) BER as a function of symbol rate for one of the channels of the QD-MLLD with modulation formats ranging from 4 to 32QAM after b2b (dash lines) and 80 km-SSMF (straight lines) transmission. (d) BER as a function of wavelengths of the 45 channels usable for transmission over 80 km-SSMF using 16QAM at 56GBd (red squares) and 32QAM at 56GBd (blue circle). (e) OSNR measurement of one of the QD-MLLD channels with the SiP modulator at 16QAM 56 GBd and 32QAM 56 GBd.

4QAM and 16QAM signals, and 80 GBd for 32QAM signals, indicating aggregate bitrates of 208 Gb/s, 416 Gb/s, and 400 Gb/s, respectively. Figure 4(d) provides an overview of the performance of all channels from the comb source. It is important to note that the results are not limited to a single wavelength as in [24], we conduct comprehensive WDM experiments, ensuring consistent and robust performance across all lines from the QD-MLLD with the SiP modulator. All channels demonstrate consistent performance, underscoring the stability of both the comb source and the SiP modulator across multiple wavelengths. As observed earlier, channels at the edges exhibit somewhat diminished performance due to lower peak power-to-noise ratios; nevertheless, their BER values remain below the SD-FEC threshold with 25% OH. Furthermore, we measured the BER as a function of OSNR measurements to further evaluate the combined performance of

Optics EXPRESS

the SiP modulator and the QD-MLLD. Figure 4(e) summarizes these results for 56 GBd with 16QAM and 32QAM. The corresponding BER values for OSNR of 22 dB and higher are below the SD-FEC threshold with 25% OH for 32QAM signaling and below the SD-FEC threshold with 20% OH for 16QAM signaling.

4. Summary

Our study demonstrates the remarkable efficiency and robustness of the QD-MLLD in coherent WDM transmission over an 80 km-SSMF. It highlights the QD-MLLD's superior frequency and phase noise performance, enabling coherent transmission with high modulation formats and symbol rates. Although our system utilizes a single polarization scheme due to limitations of the SHF QAM transmitter, it can be readily upgraded to a dual-polarization setup, effectively doubling the net bitrates achieved. Assuming the transmitter and receiver are not bandwidth limited, the performance limits of such comb sources would be mainly determined by the RIN, the optical linewidth, and the SNR. These factors have a great impact on determining the highest symbol rate and modulation format that the QD-MLLDs can achieve. One of the key takeaways from our investigation is the adaptability of such comb sources. All the measured BER values across the comb source channels consistently fall within acceptable FEC thresholds. We demonstrate the QD-MLLD's flexibility by showcasing that it can be programmed using a programmable optical filter to manipulate the frequency spacing between the comb lines, to match the target application requirements. Additionally, our findings indicate that the QD-MLLD can perform both as LOs and signal carriers, and its performance closely matches that of the commercial narrow-linewidth ITLA, further emphasizing its competitive edge. Another notable aspect is the potential for hybrid integration with silicon photonics. Our transmission experiments successfully demonstrate that the QD-MLLD can function very well with a SiP modulator, opening doors for hybrid integration in future optical transceiver modems for coherent optical communication systems, whether for short or long-distance fiber transmissions. Our study culminates in the impressive achievement of utilizing the QD-MLLD to attain a high modulation format of 64QAM at an impressive symbol rate of 80 GBd, resulting in a net bitrate of 447.8 Gb/s per channel. In summary, the QD-MLLD emerges as a highly promising technology for the realm of coherent optical communication. Its efficient operation, wide comb spectrum, compatibility with silicon photonics, and competitive performance, along with its ability to support high symbol rates, position it as an asset in advancing optical communication systems, both for short and long-distance applications.

Funding. National Research Council Canada; Natural Sciences and Engineering Research Council of Canada; Fonds de recherche du Québec – Nature et technologies.

Acknowledgments. The authors would like to acknowledge the support of National Challenge Program "High Throughput and Secure Networks (HTSN)" from the National Research Council Canada.

Disclosures. The authors declare no conflicts of interest.

Data availability. Data underlying the results presented in this paper are not available at this time but may be obtained from the authors upon reasonable request.

References

1. P. J. Winzer, D. T. Neilson, and A. R. Chraplyvy, "Fiber-optic transmission and networking: the previous 20 and the next 20 years [Invited]," Opt. Express **26**(18), 24190–24239 (2018).
2. V. Torres-Company, J. Schröder, A. Fülöp, *et al.*, "Laser frequency combs for coherent optical communications," J. Lightwave Technol. **37**(7), 1663–1670 (2019).
3. P. Marin-Palomo, J. N. Kemal, T. J. Kippenberg, *et al.*, "Performance of chip-scale optical frequency comb generators in coherent WDM communications," Opt. Express **28**(9), 12897–12910 (2020).
4. S. Liu, X. Wu, D. Jung, *et al.*, "High-channel-count 20 GHz passively mode-locked quantum dot laser directly grown on Si with 4.1 Tbit/s transmission capacity," Optica **6**(2), 128–134 (2019).
5. Z. Lu, J. Liu, L. Mao, *et al.*, "*12.032 Tbit/s coherent transmission using an ultra-narrow linewidth qantum dot 34.46 GHz C-Band coherent comb laser*" (SPIE, 2019).
6. P. Marin-Palomo, J. N. Kemal, P. Trocha, *et al.*, "Comb-based WDM transmission at 10 Tbit/s using a DC-driven quantum-dash mode-locked laser diode," Opt. Express **27**(22), 31110–31129 (2019).

Optics EXPRESS

7. P. Marin-Palomo, J. N. Kemal, M. Karpov, *et al.*, "Microresonator-based solitons for massively parallel coherent optical communications," Nature **546**(7657), 274–279 (2017).
8. S. Fujii, S. Tanaka, T. Ohtsuka, *et al.*, "Dissipative Kerr soliton microcombs for FEC-free optical communications over 100 channels," Opt. Express **30**(2), 1351–1364 (2022).
9. J. Pfeifle, V. Brasch, M. Lauermann, *et al.*, "Coherent terabit communications with microresonator Kerr frequency combs," Nat. Photonics **8**(5), 375–380 (2014).
10. B. Corcoran, M. Tan, X. Xu, *et al.*, "Ultra-dense optical data transmission over standard fibre with a single chip source," Nat. Commun. **11**(1), 2568 (2020).
11. Y. Geng, H. Zhou, X. Han, *et al.*, "Coherent optical communications using coherence-cloned Kerr soliton microcombs," Nat. Commun. **13**(1), 1070 (2022).
12. H. Zhou, Y. Geng, W. Cui, *et al.*, "Soliton bursts and deterministic dissipative Kerr soliton generation in auxiliary-assisted microcavities," Light: Sci. Appl. **8**(1), 50 (2019).
13. J. Pfeifle, V. Vujicic, R. T. Watts, *et al.*, "Flexible terabit/s Nyquist-WDM super-channels using a gain-switched comb source," Opt. Express **23**(2), 724–738 (2015).
14. P. M. Anandarajah, R. Maher, Y. Q. Xu, *et al.*, "Generation of coherent multicarrier signals by gain switching of discrete mode lasers," IEEE Photonics J. **3**(1), 112–122 (2011).
15. Y. Cui, Z. Wang, Y. Xu, *et al.*, "Generation of flat optical frequency comb using cascaded pms with combined harmonics," IEEE Photon. Technol. Lett. **34**(9), 490–493 (2022).
16. H. Sun, M. Khalil, Z. Wang, *et al.*, "Recent progress in integrated electro-optic frequency comb generation," J. Semicond. **42**(4), 041301 (2021).
17. Y. Mao, G. Liu, K. Zeb, *et al.*, "Ultralow noise and timing jitter semiconductor quantum-dot passively mode-locked laser for terabit/s optical networks," Photonics **9**(10), 695 (2022).
18. V. Vujicic, C. Calò, R. Watts, *et al.*, "Quantum dash mode-locked lasers for data centre applications," IEEE J. Select. Topics Quantum Electron. **21**(6), 53–60 (2015).
19. J. N. Kemal, P. Marin-Palomo, V. Panapakkam, *et al.*, "Coherent WDM transmission using quantum-dash mode-locked laser diodes as multi-wavelength source and local oscillator," Opt. Express **27**(22), 31164–31175 (2019).
20. H. Asghar, W. Wei, P. Kumar, *et al.*, "Stabilization of self-mode-locked quantum dash lasers by symmetric dual-loop optical feedback," Opt. Express **26**(4), 4581–4592 (2018).
21. Z. G. Lu, J. R. Liu, P. J. Poole, *et al.*, "Ultra-narrow linewidth quantum dot coherent comb lasers with self-injection feedback locking," Opt. Express **26**(9), 11909–11914 (2018).
22. E. Berikaa, M. S. Alam, A. Samani, *et al.*, eds. (Optica Publishing Group, 2022), paper Th4A.5.
23. E. Berikaa, M. S. Alam, A. Samani, *et al.*, "Transmission of 100 gbaud 64qam using an all-silicon iq modulator," in *Conference on Lasers and Electro-Optics* (2022), pp. 1–2.
24. E. Berikaa, M. S. Alam, A. Samani, *et al.*, "Silicon photonic single-segment iq modulator for net 1 tbps/λ transmission using all-electronic equalization," J. Lightwave Technol. **41**(4), 1192–1199 (2023).
25. G. Liu, P. J. Poole, Z. Lu, *et al.*, "Mode-locking and noise characteristics of InAs/InP quantum dash/dot lasers," J. Lightwave Technol. **41**(13), 4262–4270 (2023).
26. Z. Lu, J. Liu, Y. Mao, *et al.*, "Quantum dash multi-wavelength lasers for Tbit/s coherent communications and 5 G wireless networks," J. Eur. Opt. Soc.-Rapid Publ. **17**(1), 9 (2021).
27. Y. Mao, Z. Lu, J. Liu, *et al.*, "Pulse timing jitter estimated from optical phase noise in mode-locked semiconductor quantum dash lasers," J. Lightwave Technol. **38**(17), 4787–4793 (2020).
28. M. Al-qadi, C. Laperle, D. Charlton, *et al.*, "Multichannel 16-QAM single-sideband transmission and Kramers–Kronig detection using a single QD-MLL as the light source," J. Lightwave Technol. **38**(22), 6163–6169 (2020).
29. M. T. A. Khan, E. Alkhazraji, A. M. Ragheb, *et al.*, "100 Gb/s Single channel transmission using injection-locked 1621 nm quantum-dash laser," IEEE Photon. Technol. Lett. **29**(6), 543–546 (2017).
30. J. N. Kemal, P. Marin-Palomo, K. Merghem, *et al.*, "32QAM WDM transmission at 12 Tbit/s using a quantum-dash mode-locked laser diode (QD-MLLD) with external-cavity feedback," Opt. Express **28**(16), 23594–23608 (2020).
31. V. Vujicic, A. Anthur, V. Panapakkam, *et al.*, "Tbit/s optical interconnects based on low linewidth quantum-dash lasers and coherent detection," in *Conference on Lasers and Electro-Optics* (2016), pp. 1–2.
32. J. Pfeifle, I. Shkarban, S. Wolf, *et al.*, "Coherent terabit communications using a quantum-dash mode-locked laser and self-homodyne detection," in *Optical Fiber Communications Conference and Exhibition* (2015), pp. 1–3.
33. M. Gay, A. O. Hare, L. Bramerie, *et al.*, "Single quantum dash mode-locked laser as a comb-generator in four-channel 112 Gbit/s WDM transmission," in *OFC* (2014), pp. 1–3.
34. T. Habruseva, S. O'Donoghue, N. Rebrova, *et al.*, "Optical linewidth of a passively mode-locked semiconductor laser," Opt. Lett. **34**(21), 3307–3309 (2009).
35. R. Rosales, K. Merghem, A. Martinez, *et al.*, "Timing jitter from the optical spectrum in semiconductor passively mode locked lasers," Opt. Express **20**(8), 9151–9160 (2012).
36. Z. Lu, J. Liu, P. J. Poole, *et al.*, "InAs/InP quantum dash semiconductor coherent comb lasers and their applications in optical networks," J. Lightwave Technol. **39**(12), 3751–3760 (2021).
37. H. Asghar, E. Sooudi, P. Kumar, *et al.*, "Optimum stabilization of self-mode-locked quantum dash lasers using dual optical feedback with improved tolerance against phase delay mismatch," Opt. Express **25**(14), 15796–15805 (2017).
38. S. J. Savory, "Digital coherent optical receivers: algorithms and subsystems," IEEE J. Select. Topics Quantum Electron. **16**(5), 1164–1179 (2010).

Optics EXPRESS

39. P. Ciblat and M. Ghogho, "Blind NLLS carrier frequency-offset estimation for QAM, PSK, and PAM modulations: performance at low SNR," IEEE Trans. Commun. **54**(10), 1725–1730 (2006).
40. I. Fatadin, D. Ives, and S. J. Savory, "Compensation of frequency offset for differentially encoded 16- and 64-QAM in the presence of laser phase noise," IEEE Photon. Technol. Lett. **22**(3), 176–178 (2010).
41. M. Khalil, E. Berikaa, M. S. Alam, *et al.*, "Performance of quantum-dash mode-locked laser diode (QD-MLLD) for data rates beyond Tb/s in WDM coherent transmission over 80 km-SMF," in *Advanced Photonics Congress* (Optica Publishing Group, 2023), paper SpW4E.2.